2,6-Diisopropylphenylphosphane: A new, bulky primary phosphane and its mono- and disilylated $Si(CH_3)_3$ and $Si(CH_3)_2$-*t*-Bu derivatives — A synthetic, crystallographic, and dynamic NMR investigation[1]

René T. Boeré and Jason D. Masuda

Abstract: The bulky primary phosphane 2,6-diisopropylphenylphosphane, $DipPH_2$, has been prepared from 1-bromo-2,6-diisopropylbenzene via the reaction of the Grignard reagent with PCl_3. The resulting mixed phosphonous dihalides $DipP(Cl,Br)_2$ are reduced with $LiAlH_4$ to yield the title compound in reasonable yield and on a synthetically useful scale. $DipPH_2$ is also used to prepare the monosilylated derivatives $DipPHSi(CH_3)_3$ and $DipPH\{Si(CH_3)_2$-*t*-Bu$\}$ as well as the disilylated compounds $DipP\{Si(CH_3)_3\}_2$ and $DipP\{Si(CH_3)_2$-*t*-Bu$\}_2$. All products have been fully characterized by IR, mass, and NMR spectroscopy. The crystal structure of $DipPH\{Si(CH_3)_2$-*t*-Bu$\}$ was determined from single-crystal diffraction data: $C_{18}H_{33}PSi$, $P2_1/c$, $Z = 4$, $a = 8.5768(10)$, $b = 28.104(3)$, $c = 8.1102(4)$ Å, $\beta = 93.341(3)°$ ($R = 0.0518$). Changes in the NMR spectrum of $DipPH\{Si(CH_3)_2$-*t*-Bu$\}$ were observed over the temperature range 178–380 K. Barrier heights were determined from the peak separation at low temperature and the coalescence points: $\Delta G^{\ddagger} \approx 40$ kJ mol^{-1} for C(aryl)—P bond rotation and ≈ 72 kJ mol^{-1} for pyramidal inversion at phosphorus.

Key words: crystal structure, 2,6-diisopropylphenyl, bulky substituents, steric congestion, dynamic NMR, primary phosphane, silyl phosphane.

Résumé : On a préparé le phosphane primaire encombré 2,6-diisopropylphénylphosphane, $DipPH_2$, à partir du 1-bromo-2,6-diisopropylbenzène, par le biais d'une réaction de Grignard avec le PCl_3. On a réduit les dihalogénures phosphoneux mixtes qui en résultent, $DipP(Cl,Br)_2$, à l'aide de $LiAlH_4$ pour obtenir le composé mentionné dans le titre avec un rendement raisonnable et à une échelle utile d'un point de vue synthétique. On a aussi utilisé le $DipPH_2$ pour préparer les dérivés monosilylés $DipPHSi(CH_3)_3$ et $DipPH\{Si(CH_3)_2$-*t*-Bu$\}$ ainsi que les produits disilylés $DipP\{Si(CH_3)_3\}_2$ et $DipP\{Si(CH_3)_2$-*t*-Bu$\}_2$. On a caractérisé tous les produits par spectroscopie IR, de masse et RMN. On a déterminé la structure cristalline du $DipPH\{Si(CH_3)_2$-*t*-Bu$\}$ par diffraction des rayons X par un cristal unique; les données pour $C_{18}H_{33}PSi$, $P2_1/c$, $Z = 4$, $a = 8{,}5768(10)$, $b = 28{,}104(3)$ et $c = 8{,}1102(4)$ Å, $\beta = 93{,}341(3)°$ ($R = 0{,}0518$). En faisant varier la température de 178 à 310 K, on a observer des changements dans le spectre RMN du $DipPH\{Si(CH_3)_2$-*t*-Bu$\}$. Les hauteurs de barrières ont été déterminées sur la base de la séparation des pics à basse température et des points de coalescence: $\Delta G^{\ddagger} \approx 40$ kJ mol^{-1} pour la rotation autour de la liaison C(aryle)—P et ≈ 72 kJ mol^{-1} pour l'inversion pyramidale au niveau du phosphore.

Mots clés : structure cristalline, 2,6-diisopropylphényle, substituants volumineux, congestion stérique, RMN dynamique, phosphane primaire, phosphane silylé.

[Traduit par la Rédaction]

Introduction

The chemistry of primary phosphanes has received much attention in recent years, and their utility in both main group chemistry (1–8) and coordination chemistry (9–18) is under active investigation. Aryl phosphanes bearing bulky substituents in the *ortho* positions have been particularly popular, as they have considerably greater stability and more

Received 14 February 2002. Published on the NRC Research Press Web site at http://canjchem.nrc.ca on 29 November 2002.

This work is dedicated to Professor Tristram Chivers in grateful acknowledgment for his constant support and sound collegial advice. Tris has served his Department, University, and Canadian chemistry impeccably and enthusiastically. His efforts have helped put main group chemistry in the forefront of Canadian science.

R.T. Boeré[2] and J.D. Masuda. Department of Chemistry and Biochemistry, University of Lethbridge, Lethbridge, AB T1K 3M4, Canada.

[1]Presented in part at the 84th Canadian Chemical Conference and Exhibition, Montreal, QC, 26–30 May 2001.
[2]Corresponding author (e-mail: boere@uleth.ca).

 DOI: 10.1139/V02-150

Scheme 1.

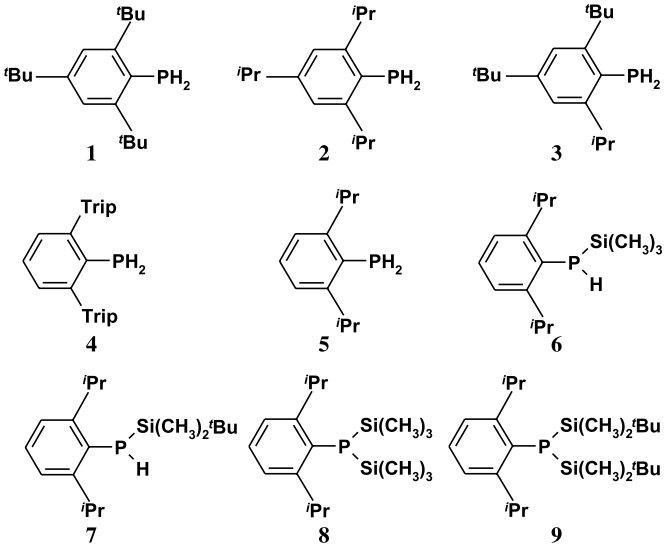

controlled reactions (3, 4, 17). The risk associated with the high toxicity of primary phosphanes such as $PhPH_2$ is also mitigated by the bulky substituents, if by nothing more than lowering the volatility of the compounds. The most commonly used bulky primary phosphane (Scheme 1) has undoubtedly been 2,4,6-tri-*tert*-butylphosphane, Mes*PH_2 (**1**) (19). The closely related 2,4,6-triisopropylphenylphosphane, TripPH_2 (**2**) is known, and its chemistry has received some attention (20). A laborious, multi-step, small-scale synthesis of 2,4-di-*tert*-butyl-6-isopropylphenylphosphane, DtbiPH_2 (**3**) has recently been reported (3). The terphenyl compound 2,6-(2,4,6-triisopropylphenyl)-phenylphosphane, TterphPH_2 (**4**) has been prepared and its crystal structure determined (4).

We have been exploiting for some time the 2,6-diisopropylphenyl (Dip) group as a bulky substituent on nitrogen, in particular for the preparation of *N*,*N′*-disubstituted amidines (21, 22) and *N*,*N′*,*N″*-trisubstituted guanidines (23). We are currently in the process of preparing directly analogous phosphorus-containing compounds via primary phosphanes (24) and we were therefore surprised to find that DipPH_2 (**5**) has not been reported heretofore in the literature and indeed there are no reports of the Dip group attached to phosphorus in any compound. At the cost of being slightly less sterically shielding, the use of *ortho* diisopropyl groups imparts to bulky substituents the advantage over *tert*-butyl of providing a wealth of stereochemical information from the ^{1}H NMR signals of the diastereotopic isopropyl groups. The 2,4,6-triisopropylphenyl (Trip) substituent has such groups, but has the disadvantage that the sterically unnecessary *para* isopropyl substituent tends to obscure the often complex and always interesting ^{1}H NMR signals of the sterically essential *ortho* isopropyl substituents. For example, in **2** the chemical shifts of the *ortho* and *para* *i*-Pr CH_3 groups are 1.23 and 1.24 ppm (20). In our experience, the *meta* and the *para* hydrogen atoms on the aromatic backbone of Dip groups tend to be well resolved and can be useful spectroscopic probes in a region of the spectrum removed from the crowded aliphatic regions. There is considerable merit in the use of the Dip substituent, and in this paper we report a practical large-scale synthesis of **5**.

Scheme 2.

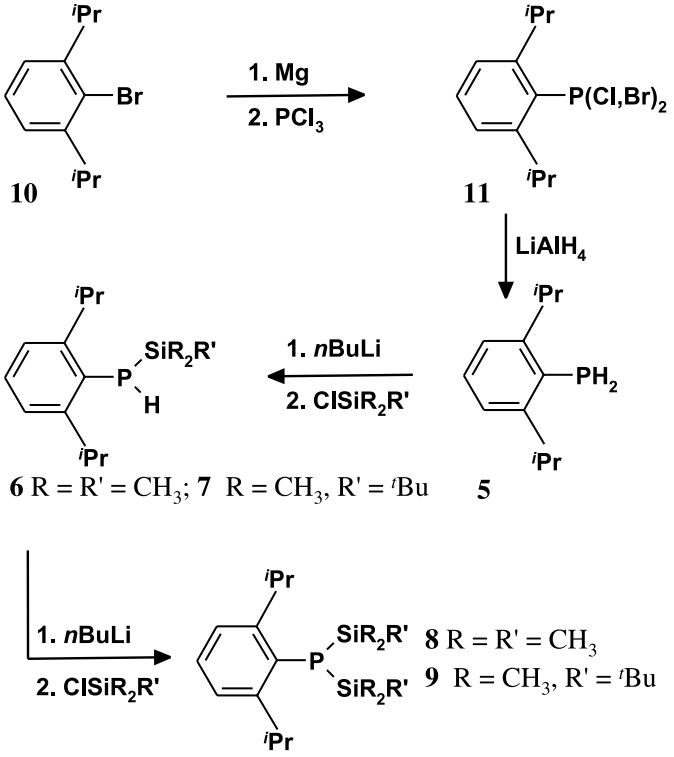

Many applications of primary phosphanes either require, or are enhanced by, replacement of one or both hydrides with silyl groups (6, 25–27). We have therefore prepared the silyl compounds Dip$PHSi(CH_3)_3$ (**6**), Dip$PH\{Si(CH_3)_2$-*t*-Bu$\}$ (**7**), Dip$P\{Si(CH_3)_3\}_2$ (**8**), and Dip$P\{Si(CH_3)_2$-*t*-Bu$\}_2$ (**9**). Although the $Si(CH_3)_3$ compounds could be prepared quite easily in sufficient purity to be of synthetic utility, it was difficult to obtain analytically pure samples of these low-melting compounds. The $Si(CH_3)_2$-*t*-Bu derivatives, on the other hand, are easily purified, crystalline solids and have been fully characterized. The strong asymmetry induced by the bulky substituent in **7** induces a dynamic process observable by NMR spectroscopy, and the results of investigations in $C_6D_5CD_3$ are reported over the temperature range 178–380 K. These solution state changes are correlated to the structure found in the solid state by a single-crystal X-ray diffraction study.

Results and discussion

Synthesis and characterization

Our synthetic route (Scheme 2) starts from DipBr (**10**) for which a large-scale synthesis has been worked out starting from the commercially available aniline (28). The Grignard reagent prepared from **10** is added to a cold solution of PCl_3 in THF. This reaction leads consistently to mixtures of all three possible halides, which co-distil as identified by their ^{31}P chemical shifts (Table 1), i.e., DipPCl_2 (**11a**), DipPClBr (**11b**), and DipPBr_2 (**11c**). Typical product distributions of the three are 1.6:2.4:1.0, which by mass balance means that virtually all of the bromide contained in the Grignard reagent ends up on phosphorus, remarkable testimony to the higher nucleophilicity of bromide versus chloride. Mixed

Table 1. ^{31}P NMR data for phosphonous dihalides, phosphanes, and silylated phosphanes[a].

No.	Compound	δ (^{31}P)	$^{1}J_{PH}$, Hz	Conditions	Reference
11a	$DipPCl_2$	+164.5	—	$CDCl_3$, RT	This work
11b	DipPClBr	+159.2	—	$CDCl_3$, RT	This work
11c	$DipPBr_2$	+151.9	—	$CDCl_3$, RT	This work
12	$DtbiPCl_2$	+164.5	—	$CDCl_3$, RT	(3)
13	$Mes*PCl_2$	+153.8	—	$CDCl_3$, RT	(3)
14	CH_3PCl_2	+191[b]	—	Not specified	(29)
15	CH_3PClBr	+190[b]	—	Not specified	(29)
16	CH_3PBr_2	+184[b]	—	Not specified	(29)
17	$PhPH_2$	–122[b]	207	Not specified	(29)
1	$Mes*PH_2$	–128.9	211	$CDCl_3$, RT	(30)
4	$TterphPH_2$	–139.8	208	$CDCl_3$, RT	(4)
3	$DtbiPH_2$	–143.9	207	$CDCl_3$, RT	(3)
18	$MesPH_2$	–153.0	204	Not specified	(17)
5	$DipPH_2$	–156.4	208	$CDCl_3$, RT	This work
2	$TripPH_2$	–158.2	203	$CDCl_3$, RT	(20)
19	$Mes*PHSi(CH_3)_3$	–130.1	212	THF	(30)
20	$Mes*PH\{Si(CH_3)_2$-*t*-Bu$\}$	–136.2	210	$CDCl_3$, RT	(30)
6	$DipPHSi(CH_3)_3$	–163.8	211	$CDCl_3$, RT	This work
21	$TripPHSiPh_3$	–169	211	C_6D_6, RT	(27)
7	$DipPH\{Si(CH_3)_2$-*t*-Bu$\}$	–175.6	212	$CDCl_3$, RT	This work
22	$PhP\{Si(CH_3)_3\}_2$	–132.8	—	Not specified	(31)
23	$Mes*P\{Si(CH_3)_3\}_2$	–142.7	—	C_6D_6, RT	(26)
8	$DipP\{Si(CH_3)_3\}_2$	–167.1	—	$CDCl_3$, RT	This work
24	$TripP\{Si(CH_3)_3\}_2$	–169.3	—	$CDCl_3$, RT	(20)
9	$DipP\{Si(CH_3)_2$-*t*-Bu$\}_2$	–193.3	—	$CDCl_3$, RT	This work

[a]Referenced to external 85% H_3PO_4; positive chemical shifts to low field (IUPAC recommendation).
[b]Sign of chemical shift adjusted to the IUPAC convention.

phosphorus halides have been observed previously, for example, in the Grignard preparation of $Mes_2P(Cl,Br)$, where Mes = 2,4,6-trimethylphenyl (32). Reduction of mixtures of **11a–c** with $LiAlH_4$ in THF yielded the phosphane **5**, as a clear, colourless liquid. It has very little odour and is quite easy to handle if stored below room temperature and under nitrogen.

Compound **5** has been fully characterized by ^{1}H, ^{31}P, and ^{13}C NMR spectroscopy, as well as by mass spectrometry and IR spectroscopy. The P–H stretch (recorded as a liquid smear) has a frequency of 2306 cm^{-1}, comparable to 2302 cm^{-1} in CH_2Cl_2 solution reported for $MesPH_2$ (**18**) (17). The ^{31}P NMR spectrum displays the expected 1:2:1 triplet with $^{1}J_{PH}$ = 208 Hz at δ –156.4. As the ^{31}P NMR spectral data for primary phosphanes with bulky substituents and their silyl derivatives are extremely scattered in the literature, we have collected values for as many derivatives as we could locate and compiled them in Table 1. A survey of these data shows that bulky primary phosphanes differ quite widely in ^{31}P chemical shift but that the $^{1}J_{PH}$ values are remarkably consistent and hence diagnostic. The ^{1}H NMR spectrum measured in $CDCl_3$ (Table 2) contains the typical aromatic and aliphatic signals of the Dip group, with the additional aspect that the isopropyl methine septet appears to be split further into doublets with 3.0 Hz coupling to phosphorus. Whether this is four-bond dipolar or through space coupling is yet to be determined. The expected doublet for the PH signal is observed. In addition, almost all the ^{13}C signals are doublets owing to coupling to the single phosphorus nucleus.

After repeated handling of a container of **5**, a new signal was detected in the ^{31}P NMR spectrum at δ –14.6, consisting of a 1:2:1 triplet with $^{1}J_{PH}$ = 477 Hz. We attribute this signal to the phosphane oxide, $DipP(O)H_2$, formed by aerobic oxidation of the phosphane, and base our assignment on the close correspondence of its NMR parameters to those of $Mes*P(O)H_2$: triplet, $^{1}J_{PH}$ = 490.7 Hz at δ –10.0 (33). Saturation of the NMR sample with dry O_2 caused the intensity of this signal to increase, consistent with our hypothesis. We have not attempted to isolate bulk phosphane oxide.

The general procedure for the preparation of the silylated compounds (Scheme 2) was to cleave P—H bonds with *n*-BuLi, then quench the resulting phosphide anions with $R_2R'SiCl$. However, either these reactions do not go to completion, or the base also cleaves P—Si bonds, so that the cleaving and quenching sequences had to be repeated more than once per step. The success of this procedure was greatly assisted by the use of ^{31}P NMR spectroscopy. Aliquots taken directly from the reaction mixture were used to assess the progress of each reaction, and in this way, we were able to prepare phosphanes **6–9** in acceptable yields. Use of the larger *t*-$BuMe_2Si$ group yielded analytically pure samples of **7** and **9**, whereas **6** and **8** always contained some minor impurities. The monosilylated phosphane **7** was

Table 2. Solution NMR data for **5**–**7** and related compounds[a].

Nuclei	Feature	**5**	**6**	**7**[b]	**8**	**9**[c]	**27**[d]	**21**[e]
$CH_3^{(A,D)}$	δ (^{1}H)	1.25	1.21	1.21	1.18	1.21	1.2	0.98
	$^3J_{HH}$ (Hz)	6.7	6.7	6.9	6.9	6.7	6.8	[f]
$CH_3^{(B,C)}$	δ (^{1}H)	= (A,D)	1.26	1.26	= (A,D)	= (A,D)	= (A,D)	1.09
	$^3J_{HH}$ (Hz)		6.7	6.7				[f]
$CH^{(1,2)}$	δ (^{1}H)	3.36	3.41	3.43	4.06	4.29	3.8	3.52
	$^3J_{HH}$ (Hz)	6.8	6.7	6.8	6.6	6.7	6.8	[f]
	$^4J_{PH}$ (Hz)	3.0	3.8	4.0			4.8	[f]
PH	δ (^{1}H)	3.84	3.46	3.51			5.6 [g]	4.44
	$^1J_{PH}$ (Hz)	207.2	210.7	211.0			216.6 [g]	211
$SiCH_3^{(E)}$	δ (^{1}H)		0.18	0.06	0.22	0.18		
	$^3J_{PH}$ (Hz)		4.3	5.3	6.1	4.3		
$SiCH_3^{(F)}$	δ (^{1}H)		= (E)	0.02	= (E)	= (E)		
	$^3J_{PH}$ (Hz)			0.9				
Si-*t*-Bu	δ (^{1}H)			1.01		0.91		
	$^3J_{PH}$ (Hz)			2.4		0.8		
H–C_4	δ (^{1}H)	7.35–7.25	7.35–7.19	7.26–7.17	7.35–7.23	7.28–7.21		
H–C_3	δ (^{1}H)	7.22–7.10	7.17–7.08	7.12–7.08	7.20–7.07	7.12–7.08		
$CH_3^{(A,D)}$	δ (^{13}C)	23.84	23.97	24.00	25.32	25.67	24.9	[f]
$CH_3^{(B,C)}$	δ (^{13}C)		24.18	24.16				[f]
$CH^{(1,2)}$	δ (^{13}C)	33.15	33.50	33.53	33.98	33.96	32.7	[f]
	$^3J_{PC}$ (Hz)	11.7	13.7	13.7	16.1	16.1	14.4	[f]
$SiCH_3^{(E)}$	δ (^{13}C)		0.67	–4.20	2.55	–1.54		
	$^2J_{CH}$ (Hz)		10.3	15.6	17.0	7.8		
$SiCH_3^{(F)}$	δ (^{13}C)			–2.93		= (C)		
C_{ipso}	δ (^{13}C)	126.04	129.21	129.04	128.29	130.44	130.4	[f]
	$^1J_{PC}$ (Hz)	13.7	20.5	21.5	14.2	9.3	15.7	[f]
C_{ortho}	δ (^{13}C)	152.08	152.03	152.47	156.44	156.57	153.0	[f]
	$^2J_{PC}$ (Hz)	9.8	9.3	9.3	10.7	11.2	11.1	[f]
C_{meta}	δ (^{13}C)	122.91	122.94	122.97	123.43	128.92	121.6	[f]
	$^3J_{PC}$ (Hz)	2.4	3.4	3.4	5.4	5.4	3.4	[f]
C_{para}	δ (^{13}C)	128.53	127.44	127.52	128.55	128.59	149.7	[f]
	$^4J_{PC}$ (Hz)				2.0	1.95		[f]
P	δ (^{31}P)	–156.4	–163.8	–175.6	–167.1	–192.9	–113.2	–169
	$^1J_{HP}$ (Hz)	207.5	210.6	212.1			214.1	211

[a]Measured in $CDCl_3$ at room temperature unless otherwise noted; label scheme:

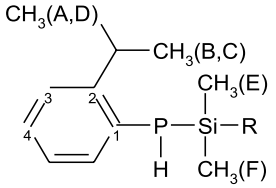

[b]*t*-Bu signals: ^{1}H NMR: 1.01 (d, $^4J_{PH}$ = 2.4 Hz, 9H). ^{13}C NMR: 27.02 (d, $^4J_{P,C}$ = 2.9 Hz, C(CH_3)$_3$), 18.70 (d, $^2J_{PC}$ = 9.8 Hz, C(CH$_3$)$_3$).
[c]*t*-Bu signals: ^{1}H NMR: 25.67 (s, C(CH_3)$_3$). ^{13}C NMR: 27.79 (d, $^4J_{PC}$ = 3.9 Hz, C(CH_3)$_3$), 20.18 (d, $^2J_{PC}$ = 20.5 Hz, C(CH$_3$)$_3$).
[d]Reference (35), measured in C_6D_6 solution at room temperature.
[e]Reference (27), measured in C_6D_6 solution at room temperature.
[f]No data provided for this parameter.
[g]Data taken from the closely related TripPHPh, **25**.

sufficiently stable to allow the investigation of its dynamic behaviour in solution by VT NMR, and this compound yielded crystals suitable for an X-ray diffraction study.

The P–H stretch of **7** (recorded as a KBr pellet) has a frequency of 2330 cm^{-1}, thus considerably higher in energy than the 2301 cm^{-1} value for **5**. ^{1}H, ^{13}C, and ^{31}P data are compiled in Tables 1 and 2. We again note the large variation in phosphorus chemical shift and the consistency of the $^1J_{PH}$ values, which are found between 203 and 212 Hz for all the trivalent P–H compounds listed in Table 1.

Structure of 7 in the solid state

The crystal structure of DipPH{Si(CH$_3$)$_2$-*t*-Bu} (**7**) was determined by X-ray diffraction at –80°C. Crystal data and structure solutions for **7** are given in Table 3, and its selected inter-atomic distances and angles in Table 4. The compound

Table 3. Crystal data for **7**.

Formula	$C_{18}H_{33}PSi$
Molecular weight	308.50
Colour, habit	Colourless, block
Dimensions (mm)	0.14 × 0.19 × 0.20
Crystal system	Monoclinic
Space Group	$P2_1/c$
a (Å)	8.5768(10)
b (Å)	28.104(3)
c (Å)	8.1102(4)
β (°)	93.341(3)
V (Å^3)	1951.6(4)
Z	4
$D_{calcd.}$ (g cm^{-3})	1.050
T (K)	193(2)
Absorption coefficient (μ) (mm^{-1})	0.194
Radiation	Mo Kα (λ=0.71073)
Crystal growth method	Sublimation
Data collection	Bruker CCD area detector; Φ and Ω scans
θ range for data collection (°)	2.38–26.41
Collection ranges	$-10 \le h \le 10$; $-29 \le k \le 35$; $-8 \le l \le 10$
Reflections collect	11 570
Independent reflections	4009 (R_{int} = 0.0618)
Absorption correction	None
Refinement	Refinement on F^2 (all data); H atoms constrained, except H(1)
Number of parameters refined	194
Final R indices [$F^2>2\sigma(F^2)$]	R_1 = 0.0518, wR_2 = 0.1114
R indices (all data)	R_1 = 0.0918, wR_2 = 0.1308
Largest diff. peak and hole (e Å^{-3})	0.338 and –0.196

Table 4. Selected bond lengths (Å) and angles (°) for **7**.

Bond lengths (Å)			
P(1)—C(1)	1.854(2)	P(1)—Si(1)	2.2681(9)
P(1)—H(1)	1.31(4)	Si(1)—C(13)	1.861(3)
Si(1)—C(14)	1.864(3)	Si(1)—C(15)	1.894(3)
C(1)—C(2)	1.415(3)	C(1)—C(9)	1.410(3)
C(2)—C(6)	1.396(3)	C(6)—C(7)	1.375(4)
C(7)—C(8)	1.374(3)	C(8)-—C(9)	1.396(3)
C(2)—C(3)	1.521(3)	C(9)—C(10)	1.521(3)
C(3)—C(4)	1.523(4)	C(3)—C(5)	1.524(3)
C(10)—C(11)	1.5331(4)	C(10)—C(12)	1.527(4)
Bond angles (°)			
C(1)-P(1)-Si(1)	104.03(7)	C(1)-P(1)-H(1)	105(2)
Si(1)-P(1)-H(1)	93(2)	C(2)-C(1)-P(1)	118.49(17)
C(1)-C(2)-C(3)	123.4(2)	C(9)-C(1)-P(1)	121.30(18)
C(2)-C(3)-C(5)	112.6(2)	C(2)-C(3)-C(4)	111.54(2)
C(9)-C(10)-C(11)	113.3(2)	C(1)-C(9)-C(10)	123.1(2)
P(1)-Si(1)-C(13)	111.97(9)	C(9)-C(10)-C(12)	110.98(2)
P(1)-Si(1)-C(15)	106.42(8)	P(1)-Si(1)-C(14)	111.20(9)

Fig. 1. An ORTEP diagram (25% probability) of the structure of **7** as found in the solid state by single-crystal X-ray crystallography. The atom numbering scheme is indicated. Hydrogen atoms are indicated by spheres of minimum radii for the sake of clarity.

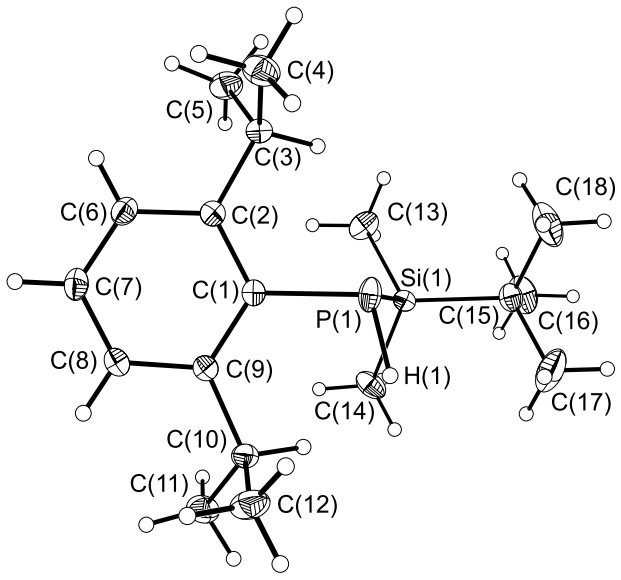

crystallizes as discrete molecules. The shortest intermolecular contacts are between H12C and H16A (2.357 Å) and H4B and H16C (2.385 Å), fractionally less than the sum of the van der Waals' radii of two H atoms. A drawing of the molecular structure and the atom-numbering scheme is presented in Fig. 1. The essential co-planarity of C(7), C(1), P(1), Si(1), C(15), and C(16) is noticeable. The RMS deviation of these atoms from a least-squares plane is 0.05 Å, with Si(1) deviating most. This molecular plane is almost exactly orthogonal to that of the aryl ring (86.38(7)° dihedral angle), with the result that the $Si(CH_3)_2$-*t*-Bu group is

Fig. 2. Calculated geometries with full optimization at the B3LYP/6–31G(*d*) level of theory for: (*a*) **5**; (*b*) **6**; (*c*) **7**; (*d*) **8**; (*e*) **9**. In each representation, the atom labelled $C_{(2)}$ is the aryl ring carbon located above the carbon $C_{(1)}$ *ipso* to phosphorus, while $C_{(9)}$ is on the lower side. See footnote (*a*) of Table 5.

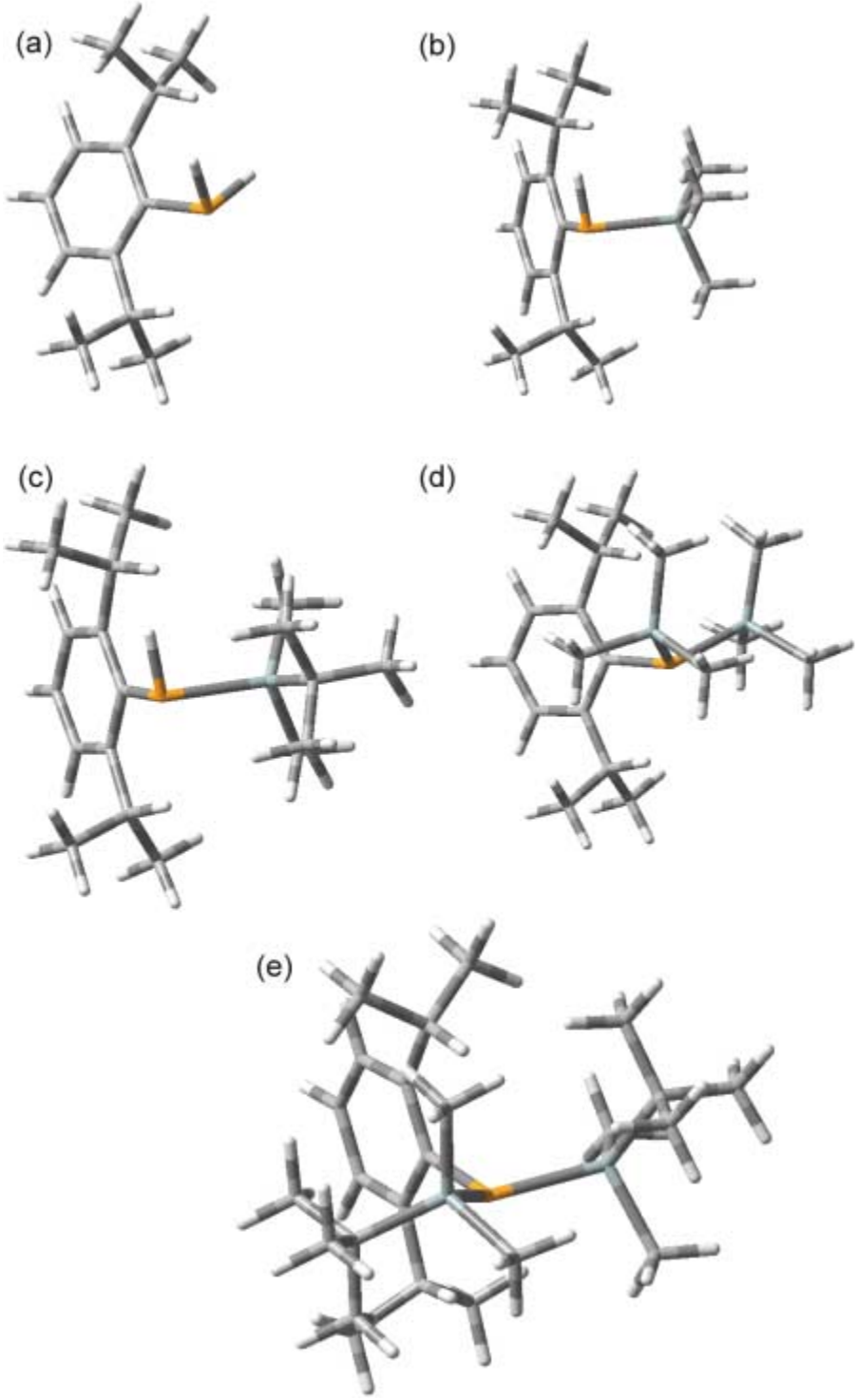

located entirely to one side of the aryl ring. Along the *t*-Bu–Si–P–aryl vector, the structure has adopted a staggered conformation about each bond. The two *ortho* isopropyl groups are oriented in the "Vee-back" conformation that we have observed in all solid-state structures determined for Dip groups (21–23, 34). However, these groups are significantly tilted such that C(5) and C(11) avoid contact with the $Si(CH_3)_2$-*t*-Bu group. In the $N\{Si(CH_3)_3\}_2$ substituted Dip group found in the structure of $Cl_3SeC_6H_2$-*i*-$Pr_2N\{Si(CH_3)_3\}_2$, where the symmetrical disilylamino group is co-planar with the aryl ring, such a tilt is not observed (34). Another noticeable feature of the structure is the large

Table 5. Calculated geometry at B3LYP/6–31G(d) level with full optimization of **5–9**.[a]

	5	6	7	8[b]	9
Distance (Å)					
$C_{(1)}$—P	1.871	1.874	1.874	1.881	1.881
$H_{(1)}$,$Si_{(1)}$—P	1.424	1.424	1.416	2.276	2.276
$H_{(2)}$,$Si_{(2)}$—P	1.425	2.298	2.307	2.276	2.296
Angle (°)					
$C_{(1)}$-P-$H_{(1)}$,$Si_{(1)}$	98.9	99.9	99.8	111.2	117.3
$C_{(1)}$-P-$H_{(2)}$,$Si_{(2)}$	99.0	105.1	103.9	111.3	111.2
$H_{(1)}$,$Si_{(1)}$-P-$H_{(2)}$,$Si_{(2)}$	93.3	95.3	96.3	113.7	117.6
∑(<P)	291.7	300.3	300.3	336.2	346.1
$C_{(2)}$-$C_{(1)}$-P	122.8	124.1	124.1	125.3	125.5
$C_{(9)}$-$C_{(1)}$-P	117.4	116.3	116.3	115.9	115.9

[a]Full geometry optimization and stationary point verification, unless otherwise indicated. Label scheme:

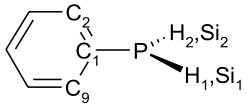

[b]Frequency calculation to verify stationary point fails.

deviations of the phosphorus (0.318(4) Å) and the *ipso* carbon C(1) (0.038(3) Å) atoms from the mean aryl plane defined by the remaining five carbon atoms. Such a deviation for the phosphorus atom has been observed previously in other "secondary" and "tertiary" phosphane structures with bulky *ortho* groups: in **23**, 0.85 Å (25), in Mes*P{OCH_2}$_2$, 0.82 Å (25), and in TripPHPh (**25**), 0.48 Å (35). However, both the structures with *ortho* isopropyl groups have the P atom displaced on the side opposite to that of the "R" substituent, while the Mes*PR_2 structures have the phosphorus pushed out on the same side of the ring as the "axial" substituent.

The sum of angles around phosphorus is only 301.5(26)°, indicative of a highly pyramidal structure at phosphorus. This is commonly observed for secondary phosphanes with bulky Trip or Mes* substituents (**25**, 304° (35); Mes*$PHSiPh_3$ (**26**), 303.9° (27)), values that are statistically indistinguishable from our results.

Calculated (gas phase) structures of 5–9

The structures of **5–9** have been calculated at the B3LYP/6–31G(d) level. Illustrations of the calculated structures are provided in Fig. 2, and some of the core geometric parameters are presented in Table 5. We started our analysis by comparing the calculated structure of **7** with that determined from the crystal structure. There is a remarkable agreement between the two, right down to the conformations adopted by the aryl isopropyl and the triorganosilyl groups. These results serve to confirm that the structure obtained in the solid state is relatively unaffected by intermolecular forces. The calculated bond lengths are 1–2% longer than the measured values, typical for the DFT methodology that we employed. However, the calculated sum of angles at phosphorus was within experimental error of the measured value.

The structures of the symmetrically substituted phosphanes **5**, **8**, and **9** are quite similar, having one substituent at each side of the aryl ring. This is unlike the results from crystallography for Mes*PX_2 derivatives, such as Mes*P{OCH_2}$_2$ or **23** (25), where both substituents are found on the same side of a (distorted) aryl ring. The pyramidal geometry at phosphorus causes a slight distortion of the bond angles, such that the angle $C_{(2)}$–$C_{(1)}$–P (the upper side for each picture in Fig. 2) is in each case somewhat larger than the angle $C_{(9)}$–$C_{(1)}$–P. The unsymmetrically substituted **6** and **7** have significantly twisted isopropyl substituents to minimize steric interactions, whereas the symmetrically substituted compounds have the isopropyl groups symmetrically disposed to the aryl rings and in the "Vee-back" conformation.

Finally, we note the great similarity in the sum of angles at phosphorus calculated for **5–7**, and the agreement of calculated and measured values for **7** (within experimental error). In contrast, when two silyl groups are attached as in **8** and **9**, the sum of angles is greatly increased (by 36–46°). We note that the calculated values of 336.2 and 346.1° are significantly greater than the average measured for Mes_3P (329.0°) from two independent molecules in the unit cell of a single crystal X-ray structure (36). However, these values are comparable to that obtained in a crystal structure for **23**, 343.2° (25)

Solution structures by NMR

The pertinent NMR data for all five phosphanes as determined in $CDCl_3$ solution have been compiled in Table 2. Data from two previously reported compounds, $TripPHCH_3$ (**27**) (35) and $TripPHSiPh_3$ (**21**) (27) have also been included to substantiate the assignment and interpretation of our results. The former is of course a secondary phosphane and hence has a ^{31}P chemical shift that is not comparable to that of ours. However, there is remarkable agreement between the NMR data for **27** and the more symmetrical of our phosphanes $DipPR_2$ (R = H, Si{CH_3}$_3$, and Si{CH_3}$_2$-*t*-Bu). This applies to the ^1H and ^{13}C parameters of the *ortho* isopropyl groups and the ^{13}C parameters of the aromatic rings, for which all the carbon nuclei except the *para* atom C_4 are doublets from coupling to phosphorus. We have also found that the silyl methyl and even the methyl hydrogen atoms of the *t*-Bu groups in **6–9** show evidence of coupling to the phosphorus nucleus.

The unsymmetrically substituted phosphanes **6** and **7** have room temperature (RT) ^1H NMR spectra in which there are two isopropyl methyl environments, but only a single CH environment. Similar effects are reported in the literature for the *ortho* isopropyl groups of **21** (27). Additionally, **7** also displays two distinct silyl methyl resonances, which have different degrees of coupling to ^{31}P, i.e., 5.3 and ~1 Hz.

VT NMR study

A variable temperature NMR study of **7** was conducted in $C_6D_5CD_3$ solution. Compound **7** is superior to **6** for this purpose, not only in being a pure crystalline material but also in possessing a pair of diastereotopic methyl groups on silicon which are direct probes for the chirality induced by the asymmetric phosphorus atom in the absence of fast pyramidal inversion. The basic spectral features of the dynamic NMR sample, which was made up in $C_6D_5CD_3$, are very similar to the RT spectrum in deuterochloroform as reported

Scheme 3.

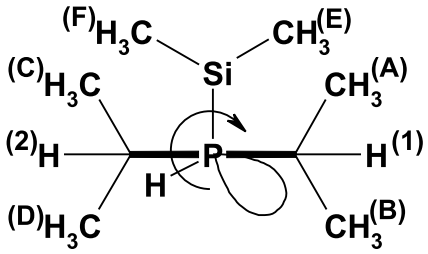

in Table 2. In Scheme 3, the molecule is viewed end-on to highlight the symmetry relationships relevant to solution dynamics (the *t*-Bu group is located in front of the Si atom, and is omitted for clarity). Figure 3 presents several traces selected from the series of spectra that illustrate the key spectral changes; full VT data have been deposited.[3]

At 380 K, the dynamic processes are in the high temperature limit. Here there is only one kind of isopropyl ($CH^{(1,2)}$ equivalent), one isopropyl methyl ($CH_3^{(A–D)}$ equivalent), and one silyl methyl group ($CH_3^{(E,F)}$ equivalent). This is achieved by a combination of rapid rotation about single bonds and rapid inversion at phosphorus. We note that the $CH_3^{(E,F)}$ signal is a phosphorus-coupled doublet with a coupling constant of ~3 Hz.

On cooling, coalescence of the $CH_3^{(A,B,C,D)}$ as well as the $CH_3^{(E,F)}$ signals occurs, and the coalesced signals become sharp at lower temperature, e.g., as in the 263 K spectrum. Here $CH_3^{(F)}$ appears as a singlet (the splitting of ~1 Hz observed in $CDCl_3$ is not resolved in the more viscous $C_6D_5CD_3$), while $CH_3^{(E)}$ is a doublet with coupling to phosphorus of ~5 Hz. The isopropyl methyl signals break into two distinct sets, labelled $CH_3^{(A,D)}$ and $CH_3^{(B,C)}$, while the $CH^{(1,2)}$ signals remain identical, as in the 380 K spectrum. These changes are consistent with slowed pyramidal inversion at the chiral phosphorus atom. Thus $CH_3^{(E)}$ and $CH_3^{(F)}$ as well as the $CH_3^{(A,D)}$ and $CH_3^{(B,C)}$ pairs become diastereotopic with respect to the chiral phosphorus atom.

Rapid rotation about single bonds has the effect of mapping $CH^{(1)}$ on $CH^{(2)}$, $CH_3^{(A)}$ on $CH_3^{(D)}$, and $CH_3^{(B)}$ on $CH_3^{(C)}$ (Scheme 3), averaging their chemical shifts in the intermediate temperature regime. Below 263 K, this rotational averaging slows down, with coalescence of the methine signals occurring at 213 K. Partial coalescence of the methyl signals is also observed at this temperature. By 178 K we had not reached the low temperature limit of this additional dynamic process, and further cooling of our solution led only to general line broadening. However, at 178 K the methine signals split up into two distinct, though broadened, signals labelled $CH^{(1)}$ and $CH^{(2)}$ (Fig. 3). We attribute this inequivalence to slowed rotation about single bonds. Other workers refer to this as slow rotation about the $C_{(aryl)}$—P bond (27), though several bond rotations are likely coupled in a molecule as sterically congested as **7**.

Using the classical expression of Gutowsky and Holm (37) with Eyring absolute rate theory (38), we can estimate the barrier heights as $\Delta G^{\ddagger}$ ~ 40 kJ mol^{-1} for rotation about single bonds and $\Delta G^{\ddagger}$ ~ 72 kJ mol^{-1} for pyramidal inversion at phosphorus. These numbers are in remarkable agreement

Fig. 3. NMR spectra of **7** at various temperatures as recorded in $C_6D_5CD_3$. Spectra were monitored at 10° intervals over the range 178 to 380 K, and in the intervening spectra to those displayed here, smooth transitions between the peaks were observed. Only the aliphatic region of each spectrum is displayed, including the silyl, the isopropyl, and the PH signals. The residual $C_6D_5CHD_2$ peak (X) is cut short in the low-temperature spectra. Similarly, the *t*-Bu peak is cut short for the middle traces.

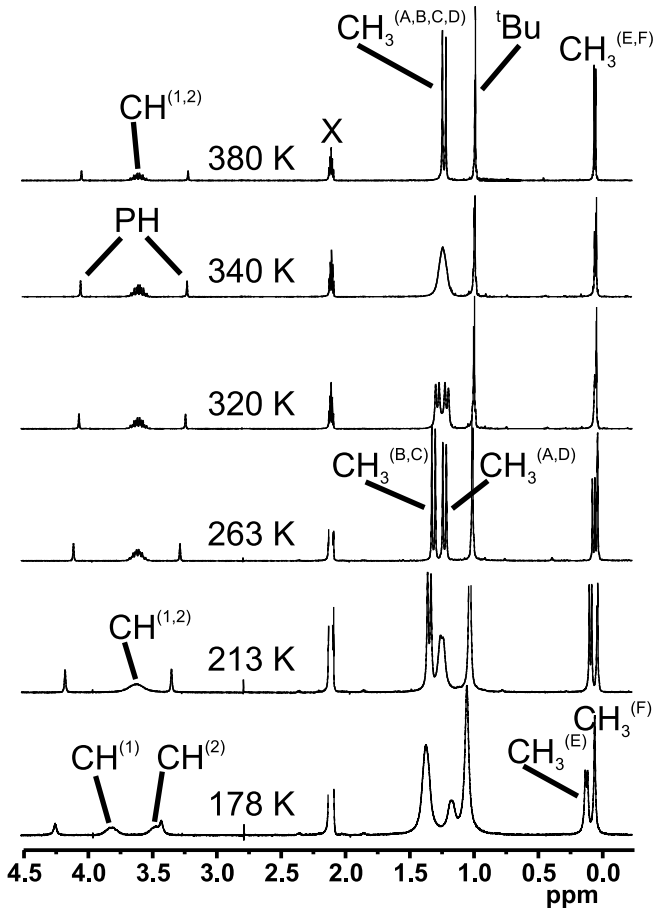

with values previously reported in a dynamic study of $TripPHSiPh_3$ (**21**): 39 kJ mol^{-1} for rotation and 71 kJ mol^{-1} for inversion (27). The assignments of the processes in **21** were made by comparison to literature data on phosphorus inversion barriers. The presence of diastereotopic groups $CH_3^{(E,F)}$ on silicon in **7** provides internal corroboration that this is the correct assignment.

Experimental

Starting materials and general procedures

All experimental procedures were performed under a nitrogen atmosphere using modified Schlenk techniques. 2,6-Diisopropylaniline (Aldrich) was distilled from KOH and stored under nitrogen prior to use. PCl_3, $SiMe_3Cl$, $SiMe_2$-*t*-BuCl (Aldrich), and HBr (Merck) were commercial products and used as received. Tetrahydrofuran was dried and distilled under a nitrogen atmosphere from sodium/benzophenone.

[3] Table S1 presents the full VT NMR Data for **7** at ~10 K intervals from 178 to 380 K.

Hexanes and pentane were dried and distilled under a nitrogen atmosphere from $LiAlH_4$. ^1H, ^{13}C, and ^{31}P NMR spectra were recorded on a Bruker AC250/Tecmag Macspect spectrometer operating at 250.13, 101.26, and 62.90 MHz, respectively. The ^1H and ^{13}C chemical shifts of $CDCl_3$ solutions were referenced to TMS and of $C_6D_5CD_3$ solutions to the residual CHD_2 pentet at δ 2.09, while ^{31}P was referenced to external 85% H_3PO_4. Infrared spectra were recorded on Bomem MB-100 or Nicolet Avatar 360 spectrometers as KBr pressed pellets (solids) or as neat liquid smears. Mass spectra were undertaken in the Department of Chemistry, University of Alberta, and elemental analyses were done by MHW Laboratories, Phoenix, Ariz. 1-Bromo-2,6-diisopropylbenzene was prepared from 2,6-diisopropylaniline by the literature method (28).

Preparation of 2,6-diisporopylphenylphosphonus mixed halide, 11

A solution of Grignard reagent was prepared from 60.0 g (247 mmol) of **10** and 6.0 g of activated magnesium turnings in 1150 mL of THF, and transferred via cannula to a solution of 67.0 g (488 mmol) PCl_3 in 200 mL THF held at –15°C. The mixture was allowed to warm to room temperature with stirring (12 h) and then heated to reflux for 2 h. Evaporation of solvent, extraction with 500 mL ether, filtering, and distillation (106–111°C, 0.5 mbar) produced 14.2 g of viscous, colourless oil. Careful integration of the ^{31}P NMR spectrum ($CDCl_3$) showed this to be the mixed phosphonous dihalides $DipPCl_2$ (**11a**) (δ 164.5, 4.5 g), DipPClBr (**11b**) (δ 159.2, 6.9 g), and $DipPBr_2$ (**11c**) (δ 151.9, 2.8 g); total molar yield 38.1%. ^1H NMR ($CDCl_3$) δ: 7.44–7.21 (m, 3H), 4.14–4.11(three sept, each with J_{HH} = 6.8 Hz, 2H), 1.34–1.29 (three d, each with J_{HH} = 6.8 Hz, 6H). ^{13}C NMR δ: 154 (d, $^2J_{PC}$ = 23 Hz), 133.49–133.41 (three d, $^3J_{PC}$ ~1 Hz), 124.97, 124.91 (two s), 31.25, (d, $^3J_{PC}$ = 27.8 Hz), 31.08, (d, $^3J_{PC}$ = 27.8 Hz), 30.89, (d, $^3J_{PC}$ = 27.3 Hz), 24.91–24.81 (three doublets, not resolved). MS (70eV) (calculated on ^{81}Br and ^{35}Cl) *m/z* (%): 354 ($[DipPBr_2]^+$, 5.5), 308 ($[DipPBrCl]^+$, 26.5), 273 ($[DipPBr]^+$, 9.8), 262 ($[DipPCl_2]^+$, 44.9), 227 ($[DipPCl]^+$, 100).

Preparation of 2,6-diisopropylphenylphosphane, 5

A solution of 10.0 g (32.7 mmol) of **11** in 150 mL anhydrous ether was transferred via cannula to a vigorously stirred suspension of 2.78 g (73.2 mmol) $LiAlH_4$ in 150 mL anhydrous ether held at –5°C. After warming to room temperature and heating to reflux for 22 h, the mixture was cooled to 0°C and treated with 53 mL of saturated aqueous NH_4Cl. The organic layer was decanted and the solids washed with 3 × 100 mL degassed ether. The combined ethereal solutions were dried, filtered, and evaporated to a milky oil. Distillation (73–85°C, 0.5 mbar) produced **5** as a clear oil (4.76 g, 24.6 mmol, 75.3% yield). IR (neat) (cm^{-1}): 3056 (w), 2961 (vs), 2868 (m), 2627 (s), 2306 (m), 1572 (w), 1461 (s), 1423 (w), 1383 (m), 1362 (m), 1247 (w), 1181 (w), 1162 (w), 1106 (w), 1086 (m), 1054 (m), 1037 (w), 923 (w), 831 (m), 792 (s), 720 (s), 499 (w). NMR, see Table 2. MS (70eV) *m/z* (%): 194.12306 ($[M]^+$, 100), 193 ($[DipPH]^+$, 44), 179 ($[C_{11}H_{16}P]^+$, 30), 161 ($[C_{12}H_{17}]^+$, 54), 152 ($[C_9H_{13}P]^+$, 44), 151 ($[C_9H_{12}P]^+$, 26), 137 ($[C_8H_{10}P]^+$, 25), 110 ($[C_6H_7P]^+$, 52), 91 ($[C_7H_7]^+$, 26). Anal. calcd. for $C_{12}H_{19}P$ (%): C 74.20, H 9.86; found: C 74.43, H 9.74.

Preparation of $DipPHSi(CH_3)_3$, 6

A solution of 28.4 mL of 1.6 M *n*-BuLi was added slowly by syringe to a vigorously stirred solution of 8.412 g (43.3 mmol) **5** in 80 mL THF held at 0°C. The now red solution was warmed to RT and stirred for 20 min, then cooled again to 0°C, whereupon 5.77 mL (45.5 mmol, 5% excess) $ClSi(CH_3)_3$ was added via syringe, followed by warming to RT and heating to reflux for 2 h. Removal of the volatile components, extraction with 100 mL hexanes, filtering, evaporation, and distillation (110–115°C, 0.5 mbar) of the residue produced 7.39 g of clear oil (29.6 mmol, 64%). NMR, see Table 2. MS (70eV) *m/z* (%): 266.16084 ($[M]^+$, 64), 193 ($[DipPH]^+$, 57), 149 ($[C_9H_{10}P]$, 14), 73 ($[SiMe_3]^+$, 100). Analytically pure material was not obtained, and all samples tended to be contaminated with very small amounts of either **5** or **8**.

Preparation of $DipPH\{Si(CH_3)_2$-*t*-Bu$\}$, 7

A solution of 4.00 g (20.6 mmol) **5** in 40 mL THF cooled to 0°C was treated with 13.5 mL (21.6 mmol, 5% excess) of 1.6 M *n*-BuLi. After warming the now yellow solution to RT for 30 min and cooling back to 0°C, 3.10 g (20.6 mmol) $ClSi(CH_3)_2$-*t*-Bu was added by syringe. After warming to RT and then refluxing for 1 h, the solution was shown by ^{31}P NMR to have 70% conversion to **7**. A further 4.5 mL of *n*-BuLi followed by 1.05 g (3.6 mmol) was used in a repeat of the above procedure. NMR indicated complete conversion at this stage. The solids remaining after evaporation of the solvent were extracted with 20 mL hexanes, filtered, evaporated, and the residue sublimed under static vacuum onto a water-cooled cold finger, yielding 3.60 g of colourless crystalline **7** (11.7 mmol, 57% yield, mp 45–51°C). X-ray quality crystals were grown by sublimation under dynamic vacuum in a three-zone tube furnace. IR (KBr pellet) (cm^{-1}): 3050(w), 2958(vs), 2925(vs), 2856(s), 2330(m), 1567(w), 1463(s), 1417(w), 1381(w), 1362(s), 1246(m), 1176(w), 1050(w), 1006(w), 938(w), 839(s), 821(s), 804(vs), 773(w), 737(vs), 680(w), 601(w), 578(w), 444(w), 430(w). NMR, see Table 2. MS (70 eV) *m/z* (%): 308.20866 ($[M]^+$, 53), 251 ($[DipP(Si(CH_3)_2]^+$, 11), 193 ($[DipPH]^+$, 15), 115 ($[(CH_3)_3CSi(CH_3)_2]^+$, 13.7), 73 ($[Si(CH_3)_3]^+$, 100). Anal. calcd. for $C_{18}H_{33}PSi$ (%): C 70.08, H 10.78; found: C 69.84, H 10.62.

Preparation of $DipP\{Si(CH_3)_3\}_2$, 8

A stirred solution prepared from 2.00 g (10.3 mmol) **5** and 20 mL THF held at 0°C was treated with 6.76 mL (10.8 mmol, 5% excess) of 1.6 M *n*-BuLi. After 20 min, the stirred orange solution was treated with 1.37 mL (10.8 mmol) $ClSi(CH_3)_3$, yielding a colourless solution with a white precipitate. ^{31}P NMR indicated that conversion to **7** was incomplete; a further 5.07 mL (8.11 mmol) of *n*-BuLi and 1.03 mL (8.11 mmol) $ClSi(CH_3)_3$ were added following the same procedure as before. ^{31}P NMR analysis indicated 75% **8** and 25% **7**. Again 5.07 mL (8.11 mmol) of *n*-BuLi and 1.03 mL (8.11 mmol) $ClSi(CH_3)_3$ were added following the same procedure and NMR analysis showed complete conversion to **8**. Evaporation of solvent, extraction with 100 mL hexanes, filtration, evaporation, and distillation of the residue (120–130°C, 0.5 mbar) gave 2.20 g of **8**, which cooled to a pasty white solid (6.5 mmol, 63% yield). IR (neat) (cm^{-1}): 3050 (m), 2957 (vs), 2867 (s), 1935 (w), 1861

(w), 1695 (w), 1651 (w), 1633 (w), 1589 (w), 1569 (m), 1557 (w), 1463 (s), 1381 (m), 1361 (m), 1304 (m), 1246 (s), 1177 (m), 1048 (m), 992 (m), 835 (s), 801 (m), 748 (m), 684 (m), 625 (m), 509 (w), 402 (w). NMR, see Table 2. MS (70eV) *m/z* (%): 338.20229 ([M]$^+$, 49), 266 ([DipPHSi(CH$_3$)$_2$]$^+$, 15), 193 ([DipPH]$^+$, 16), 147 ([C$_{11}$H$_{15}$]$^+$, 13.7), 73 ([Si(CH$_3$)$_3$]$^+$, 100). An analytically pure sample was not obtained.

Preparation of DipP{Si(CH$_3$)$_2$-*t*-Bu}$_2$, 9

A solution of 2.00 g (10.3 mmol) **5** in 20 mL THF held at 0°C was treated with 6.43 mL (10.29 mmol) of 1.6 M *n*-BuLi. After warming to RT, the yellow solution was cooled again and treated with 1.55 g (10.29 mmol) ClSi(CH$_3$)$_2$-*t*-Bu. The faint yellow solution was allowed to warm to room temperature over 30 min. Cooling again in an ice bath and treating with another 6.43 mL of 1.6 M *n*-BuLi gave an orange solution. Again 1.55 g ClSi{CH$_3$)$_2$-*t*-Bu} was added after warming the reaction mixture to room temperature and cooling to 0°C. The faint yellow solution was then heated to reflux for 12 h and ^{31}P NMR analysis showed complete conversion to **9**. Evaporation of solvent, extraction into 30 mL pentane, filtering, and evaporation yielded a white solid, which was purified by sublimation under dynamic vacuum onto a water-cooled cold finger to give 2.934 g of a white crystalline **9** (7.7 mmol, 75% yield, mp 57–62°C). IR (KBr pellet) (cm^{-1}): 3047 (w), 2958 (vs), 2929 (vs), 2894 (s), 2857 (s), 2569 (w), 1471 (m), 1460 (m), 1403 (w), 1388 (m), 1380 (m), 1360 (m), 1251 (s), 1245 (s), 1177 (w), 1048 (w), 1024 (w), 1005 (w), 834 (vs), 820 (s), 794 (vs), 760 (s), 742 (m), 681 (w), 670 (m), 660 (w), 575 (w), 470 (w), 408 (w). NMR, see Table 2. MS (70 eV) *m/z* (%): 422.29533 ([M]$^+$, 30), 251 ([M – *t*-Bu]$^+$, 11), 73 ([Si(CH$_3$)$_3$], 100). Anal. calcd. for C$_{24}$H$_{47}$PSi$_2$ (%): C 68.18, H 11.21; found: C 67.99, H 10.94.

X-ray diffraction analysis of DipPH{Si(CH$_3$)$_2$-*t*-Bu}, 7

The crystal structure of **7** was determined using a Bruker instrument fitted with a SMART 1000 area detector. Experimental details are summarized in Table 3. The structure was solved by direct methods using SHELXS-97 (39) and refined by full-matrix least-squares on F^2 against all reflections using SHELXL-97 (40). Neutral atom scattering factors are from *International Tables for X-ray Crystallography*, Vol. C. The weighting scheme used was $w = 1/[\sigma^2(c) + (0.0705P)^2]$, where $P = (F_o^2 + 2F_c^2)/3$. The non-hydrogen atoms were refined anisotropically, and the H atoms on C were refined using a riding model (C—H = 0.95 Å). The H atom attached to P was refined freely. Additional crystallographic details have been deposited.[4]

Electronic structure calculations

The structures of the full geometries of **5–9** were optimized by DFT methods, using the B3LYP hybrid function and the 6–31G(d) basis set, as implemented in the Gaussian98 suite of programs (41) running on AMD K7 computers under Windows 2000 or on four processor Compaq Alpha ES40 or ES45 workstations. Full frequency calculations were performed on all models, and stationary states were confirmed by the absence of imaginary frequencies. In the case of **8** the frequency calculation was unsuccessful, but the strong agreement with the structures of other members of the series provides confidence in the calculated structure.

Conclusions

A new bulky phosphane and two mono- as well as two disilyl derivatives were prepared by routes that provide these materials in synthetically useful quantities. The silyl compounds as well as the phosphane itself are expected to be useful synthons for both main group and transition metal chemistry. We have identified a further example of dynamic effects in compounds of the general class ArPHSiR$_3$ where both the aryl group and silicon bear sterically congested substituents. Studies on the utility of **5–9** as synthons are ongoing in our laboratory.

Acknowledgments

We thank the Natural Sciences and Engineering Research Council of Canada (NSERC) and the University of Lethbridge for financial support (R.T.B.). We thank Dr. Bob Macdonald, Department of Chemistry, University of Alberta, for the collection of the intensity data for the X-ray diffraction study, and Meg O'Shea for performing the DFT calculations. Access to the Multimedia Advanced Computation Infrastructure (MACI) Alpha cluster at the University of Calgary is gratefully acknowledged. We thank Dr. Paul Hazendonk for helpful discussions, and anonymous referees for useful suggestions.

References

1. R.A. Berrigan, D.K. Russell, W. Henderson, M.T. Leach, B.K. Nicholson, G. Woodward, and C. Harris. New J. Chem. **25**, 322 (2001).
2. C. Frenzel, F. Somoza, S. Blaurock, and E. Hey-Hawkins. J. Chem. Soc. Dalton Trans. 3115 (2001).
3. K. Toyota, Y. Matsushita, N. Shinohara, and M. Yoshifuji. Heteroat. Chem. **12**, 418 (2001).
4. B. Twamley, C-S. Hwang, N.J. Hardman, and P.P. Power. J. Organomet. Chem. **609**, 152 (2000).
5. H. Dorn, R.A. Singh, J.A. Massey, J.M. Nelson, C.A. Jaska, A.J. Lough, and I. Manners. J. Am. Chem. Soc. **122**, 6669 (2000).
6. M. Driess, S. Kuntz, C. Monse, and K. Merz. Chem. Eur. J. **6**, 4343 (2000).
7. G.W. Rabe, H. Heise, L.M. Liable-Sands, I.A. Guzei, and A.L. Rheingold. J. Chem. Soc. Dalton Trans. 1863 (2000).
8. G.W. Rabe, S. Kheradmandan, and G.P.A. Yap. Inorg. Chem. **37**, 6541 (1998).

[4] Supplementary data (Tables S1–S7) may be purchased from the Depository of Unpublished Data, Document Delivery, CISTI, National Research Council Canada, Ottawa, ON K1A 0S2, Canada (http://www.nrc.ca/cisti/irm/unpub_e.shtml for information on ordering electronically). CCDC 186019 contain the supplementary data for this paper. These data can be obtained, free of charge, via www.ccdc.cam.ac.uk/conts/retrieving.html (or from the Cambridge Crystallographic Data Centre, 12 Union Road, Cambridge, U.K.; fax +44 1223 336033; or deposit@ccdc.cam.ac.uk).

9. N.J. Goodwin, W. Henderson, B.K. Nicholson, J. Fawcett, and D.R. Russell. J. Chem. Soc. Dalton Trans. 1785 (1999).
10. S.J.A. Pope and G. Reid. J. Chem. Soc. Dalton Trans. 1615 (1999).
11. J.T. Scheper, K.C. Jayaratne, L.M. Liable-Sands, G.P.A. Yap, A.L. Rheingold, and C.H. Winter. Inorg. Chem. **38**, 4354 (1999).
12. T. Campbell, A.M. Gibson, R. Hart, S.D. Orchard, S.J.A. Pope, and G. Reid. J. Organomet. Chem. **592**, 296 (1999).
13. D.J. Darensbourg, J.D. Draper, B.J. Frost, and J.H. Reibenspies. Inorg. Chem. **38**, 4705 (1999).
14. W. Malisch, K. Thirase, F.J. Rehmann, J. Reising, and N. Gunzelmann. Eur. J. Inorg. Chem. 1589 (1998).
15. G.A.A. Hadi, K. Fromm, S. Blaurock, S. Jelonek, and E. Hey-Hawkins. Polyhedron, **16**, 721 (1997).
16. R. Felsberg, S. Blaurock, S. Jelonek, T. Gelbrich, R. Kirmse, A. Voigt, and E. Hey-Hawkins. Chem. Ber. **130**, 807 (1997).
17. I.V. Kourkine, S.V. Maslennikov, R. Ditchfield, D.S. Glueck, G.P.A. Yap, L.M. Liable-Sands, and A.L. Rheingold. Inorg. Chem. **35**, 6708 (1996).
18. J. Ho, T.L. Breen, A. Ozarowski, and D.W. Stephan. Inorg. Chem. **33**, 865 (1994).
19. A.H. Cowley, N.C. Norman, and M. Pakulski. Inorg. Synth. **27**, 235 (1990).
20. Y. v.d. Winkel, H.M.M. Bastiaans, and F. Bickelhaupt. J. Organomet. Chem. **405**, 183 (1991).
21. R.T. Boeré, V. Klassen, and G. Wolmershäuser. J. Chem. Soc. Dalton Trans. 4147 (1998).
22. R.T. Boeré, V. Klassen, and G. Wolmershäuser. Can. J. Chem. **78**, 583 (2000).
23. R.E. Boeré, R.T. Boeré, J. Masuda, and G. Wolmershäuser. Can. J. Chem. **78**, 1613 (2000).
24. R.T. Boeré and J.D. Masuda. Abstract #902. 84th Canadian Chemical Conference and Exhibition, Montreal, May 26–30, 2001.
25. A.H. Cowley, M. Pakulski, and N.C. Norman. Polyhedron, **6**, 915 (1987).
26. M. Yoshifuji, K. Shimura, and K. Toyota. Bull. Chem. Soc. Jpn, **67**, 1980 (1994).
27. M.A. Petrie and P.P. Power. J. Chem. Soc. Dalton Trans. 1737 (1993).
28. R.R. Shrock, M. Wesolek, A.H. Liu, K.C. Wallance, and J.C. Dewan. Inorg. Chem. **27**, 2050 (1988).
29. V. Mark, C.H. Dungan, M.M. Crutchfield, and J.R. Van Wazer. Top. Phosphorus Chem. **5**, 227 (1967).
30. M. Yoshifuji, K. Toyota, K. Shibayama, and N. Inamoto. Chem. Lett. 1653 (1983).
31. R. Appel and K. Geisler. J. Organomet. Chem. **112**, 61 (1976).
32. J.B. Lambert and J-H. So. J. Org. Chem. **56**, 5960 (1991).
33. M. Yoshifuji, K. Shibayama, K. Toyota, and N. Inamoto. Tetrahedron Lett. **24**, 4227 (1983).
34. A. Maaninen, R.T. Boeré, T. Chivers, and M. Parvez. Z. Naturforsch. B Chem Sci. **54**, 1170 (1999).
35. D.J. Brauer, F. Bitterer, F. Dörrenbach, G. Heßler, O. Stelzer, C. Krüger, and F. Lutz. Z. Naturforsch. B Chem Sci. **51**, 1183 (1996).
36. J.F. Blount, C.A. Marynoff, and K. Mislow. Tettrahedron Lett. 913 (1975).
37. H.S. Gutowsky and C.H. Holm. J. Chem. Phys. **25**, 1228 (1956).
38. J. Sandström. Dynamic NMR spectroscopy. Academic Press, London. 1982.
39. G. Sheldrick. 1997. SHELXS-97 [computer program]. University of Göttingen, Göttingen, Germany.
40. G. Sheldrick. 1997. SHELXL-97 [computer program]. University of Göttingen, Göttingen, Germany.
41. M.J. Frisch, G.W. Trucks, H.B. Schlegel, G.E. Scuseria, M.A. Robb, J.R. Cheeseman, V.G. Zakrzewski, J.A. Montgomery, Jr., R.E. Stratmann, J.C. Burant, S. Dapprich, J.M. Millam, A.D. Daniels, K.N. Kudin, M.C. Strain, O. Farkas, J. Tomasi, V. Barone, M. Cossi, R. Cammi, B. Mennucci, C. Pomelli, C. Adamo, S. Clifford, J. Ochterski, G.A. Petersson, P.Y. Ayala, Q. Cui, K. Morokuma, D.K. Malick, A.D. Rabuck, K. Raghavachari, J.B. Foresman, J. Cioslowski, J.V. Ortiz, A.G. Baboul, B.B. Stefanov, G. Liu, A. Liashenko, P. Piskorz, I. Komaromi, R. Gomperts, R.L. Martin, D.J. Fox, T. Keith, M.A. Al-Laham, C.Y. Peng, A. Nanayakkara, M. Challacombe, P.M.W. Gill, B. Johnson, W. Chen, M.W. Wong, J.L. Andres, C. Gonzalez, M. Head-Gordon, E. S. Replogle, and J.A. Pople. 1998. Gaussian 98 [computer program]. Revision A.9. Gaussian, Inc., Pittsburgh, Pa.